INTERNATIONAL JOURNAL OF INTEGRATED ENGINEERING
ISSN: 2229-838X e-ISSN: 2600-7916

IJIE

Vol. 17 No. 8 (2025) 139-147
https://publisher.uthm.edu.my/ojs/index.php/ijie

Energy Absorption and Failure Mechanism of Aluminium Bi-tubular Cones under Axial Compression

Asad A Khalid[1]*, Murhamdilah Murni[1]

[1] *Department of Mechanical Engineering, Faculty of Engineering, Universiti Teknologi Brunei, Tungku Link, Road,Brunei Muara BE1410, BRUNEI*

*Corresponding Author: asad.khalid@utb.edu.bn
DOI: https://doi.org/10.30880/ijie.2025.17.08.013

Article Info

Received: 1 June 2025
Accepted: 20 November 2025
Available online: 31 December 2025

Keywords

Energy absorption, failure mechanism, tubular cones, axial compression

Abstract

Thin-walled tubes of circular and noncircular cross-sections are increasingly used as energy absorbers in many applications. The most important target of the designers in automotive manufacturing is to develop a structural component that can sustain high loads and absorb high energy to provide more safety to the passengers and the driver of the vehicle. In addition, to protect vehicle components from catastrophic failure during low or high velocity crush conditions. Crashworthiness performance of the energy absorber component under axial loading depends on the fracture mechanism by which the component collapses. Fracture mechanism of thin-walled metal and composite tubes influenced by the cross-section, design parameters, and material used. In the current research, finite element analysis on aluminium bi-tubular cone components under axial loading was conducted. Combined cone-tube consists of a 56 mm tube diameter and 65.63 mm cone top diameter with cone semi-apical angles of 5°, 10°, 15°, 20° and 25° were analysed under axial loading. The effect of cone semi-vertex angle (α) for cone-cone, cone-tube, and tube-tube arrangements on the load-displacement characteristics and the absorbed energy was investigated. Crashworthiness analysis was conducted on the fractured bi-tubular component. Results presented that the crushing load and energy absorption of the bi-tubular cone-tube and cone-cone enhanced with increasing cone angle from 5° to 15°. An additional increase in the cone angle up to 25°, decreased the energy absorption, and the bi-tubular components sustained lower loads. Initial crush load of the cone-tube bi-tubular component increased from 20.04 kN to 30.50 kN with increasing cone angle from 5° to 15°. The tested bi-tubes fractured by progressive folding, accompanied by buckling that resulted in a concertina plastic failure mode, followed by a non-symmetric diamond failure mode.

1. Introduction

Thin-walled tubes made of metals and composite materials under compression loading were considered in many applications for the crashworthiness of energy absorption equipment [1]. Absorbed Energy and failure mechanism of metal tubes subjected to axial load are affected by the design parameters and material type used [2]. The demand for using aluminum material in the automotive industry is increasing where the manufacturers consider the environmental factors. The weight of the vehicle can be reduced by 25% by using an aluminum body structure compared to steel materials [3],[4].

This is an open access article under the CC BY-NC-SA 4.0 license.

Axial compression of hybrid aluminum-composite tubes has been studied by El-Hage *et al*. [5]. The authors found that folding of hybrid tubes with 45° chamfer started at a higher force than aluminum tubes [5]. In another study, El-Hage *et al.* [6] suggested an equation to estimate the average compression load of hybrid aluminum-glass tubes. The initial folding load, average load, and absorbed energy of the aluminum tubes were enhanced when using a hybrid material [6].

Several researchers investigated the crashworthiness performance of bi-tubes of various section shapes, such as square [7],[8] circular [9], triangular [10], and hybrid bi-tubular components [11]. Combined square tubes under axial load were investigated by Haghi *et al*. [7]. The authors stated that using combined square tubes of diamond and parallel arrangements under axial compression increased the absorbed energy.

The behavior of tapered thin-walled rectangular tubes subjected to static and dynamic compression was investigated by Nagel *et al.* [12]. The authors found that increasing the taper angle increased the crush efficiency [12]. In another study, they studied the influence of tapered tube wall thickness and the number of tapered rectangular tubes and found that the absorbed energy of tapered tubes is clearly affected by wall thickness [13]. Also, the authors concluded that the average crush force and absorbed energy increase obviously with increasing the number of tapered tubes under compression [13]. Khalid *et al*. [14] investigated the performance of cotton and glass/ epoxy cones under axial compression. The authors concluded that increasing the crush distance increased the load gradually for both materials investigated. The increase in cone angle from 5° to 20° of composite cones increased the energy absorption, and the cones sustained higher loads [14].

For the purpose of enhancing the energy absorption and performance of the energy absorber under axial crushing, and to get a lighter-weight energy absorber, the crashworthiness performance of aluminum bi-tubes of cone-cone and cone-tube components of different cone semi-vertex angles was selected for this investigation. Based on the literature review conducted on the crashworthiness of energy absorbers, the performance of combined cones and cone-tube components of different cone angles has not yet been investigated.

The current research aims to investigate the folding characteristics, absorbed energy, and failure mechanism of bi-tubular aluminum cone-tube and cone-cone using cone semi-apical angles ranging from 5° to 25° subjected to axial load. The research also aims to examine the crashworthiness of the fractured bi-tubes.

2. Methodology

2.1 Finite Element Analysis

An analysis of the behavior of aluminum bi-tubular cone-tube specimens subjected to axial loading was performed using LS-DYNA finite element analysis software [15]. The LS DYNA software is prepared for dynamic analysis. Scaling up the mass of the tube and the cone by a factor of 1000 has been used to conduct the quasi–static analysis. This process decreases the number of steps necessary to enhance computation efficiency. The ratio of the kinetic energy to the internal energy was kept less than 5% throughout the axial compression [16-18]. The geometrical arrangement of bi-tubes is presented in Figure 1. Where the wall thickness is t., the top and bottom diameters are respectively Dt and Db.

Dimensions of bi-tubes for this investigation are shown in Table 1. Height and wall thickness of the cone were maintained as 120 mm and 3 mm, respectively. As shown in the model type, the first terms T and C represent the tube and cone, respectively. The last term is a number that represents the specimen's cone semi-apical angle.

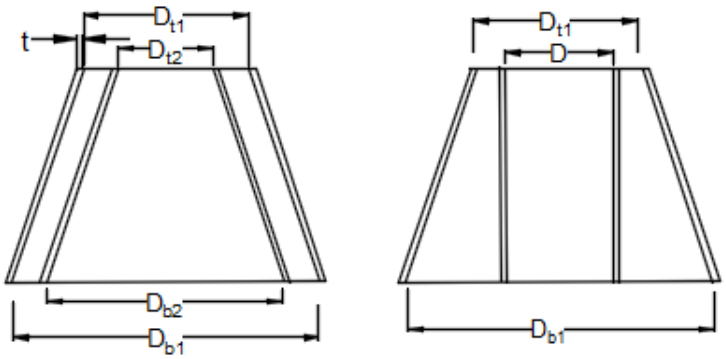

Fig. 1 *Geometrical arrangement of bi-tubes (a) Cone-cone; (b) Cone-tube*

Int. Journal of Integrated Engineering Vol. 17 No. 8 (2025) p. 139-147

Table 1 *Dimensions of aluminium bi-tubular cone and cone-tube*

Model type	Cone					Tube Inner Diameter D, [mm]
	Outer cone			Inner cone		
	Semi-apical angle α, [deg]	Top diameter D_{t1}, [mm]	Bottom diameter D_{b1}, mm]	Top diameter D_{t2}, [mm]	Bottom Diameter D_{b2}, [mm]	
T0	-	-	-	-	-	56
TT0	-	-	-	-	-	56,65.63
C5	5	65.63	86.62	-	-	-
CT5	5	65.63	86.62	-	-	56
CC5	5	65.63	86.62	56	76.98	-
C10	10	65.63	107.95	-	-	-
CT10	10	65.63	107.95	-	-	56
CC10	10	65.63	107.95	56	98.32	-
C15	15	65.63	129.94	-	-	-
CT15	15	65.63	129.94	-	-	56
CC15	15	65.63	129.94	56	120.31	-
C20	20	65.63	152.98	-	-	-
CT20	20	65.63	152.98	-	-	56
CC20	20	65.63	152.98	56	143.35	-
C25	25	65.63	177.54	-	-	
CT25	25	65.63	177.54	-	-	56
CC25	25	65.63	177.54	56	167.91	-

2.2 Element Type and Material Model

Belytschko-Tsay quadrilateral shell elements are used to model the Bi-tubes, upper and lower plates. [19]. Aluminum tube and cone are represented by the MAT_024_PIECEWISE_LINEAR_PLASTICITY material model. While the upper and lower plates are represented by the MAT_020_RIGID material model. Aluminum specific mass, modulus of elasticity, and Poisson's ratio are respectively 2700 kg/m^3, 69e9 N/m^2, and 0.3. The rigid plates' properties are 7830 kg/m^3, 207e9 N/m^{2,} and 0.3, respectively.

2.3 Boundary Constraints

The cone and tube models were placed in space, separating the two plates; shell elements were used to model all components. The finite element model is shown in Figure 2. The upper rigid plate was permitted to move vertically, while the lower rigid plate was completely restricted from motion. The BOUNDARY_PRESCRIBED_MOTION_RIGID keyword is implemented to provide motion to the upper plate downward. Contact between rigid plates and bi-tubes is represented by CONTACT_AUTOMATIC_SURFACE_TO_SURFACE. Interpenetration of cone and tube walls during progressive folding is restrained throughout by releasing the penetrated nodes by using CONTACT_AUTOMATIC_SINGLE_SURFACE.

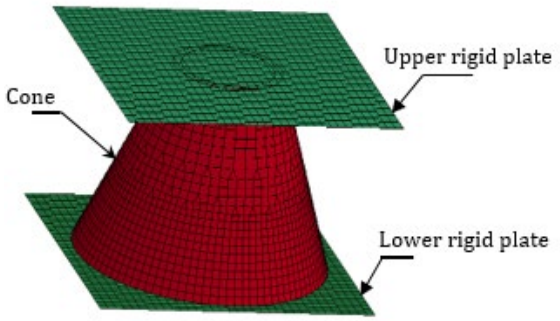

Fig. 2 *Finite element model of the bi-tubular cone-tube and rigid plates*

3. Results

3.1 Model Validation

Finite element analysis on cone models using LS-Dyna was validated with the experimental results conducted by Kathiresan *et al.* [20] for an aluminum cone subjected to axial crushing. Cone semi-vertex angle, length, and thickness were 18°, 95 mm, and 0.95 mm, respectively. Poisson's ratio, elastic modulus, yield strength, and density of aluminum material were v= 0.3. E = 70 GPa, 55 MPa, and ρ = 2710 kg/m^3, respectively.

Aluminum material is modelled using MAT_024_PIECEWISE_LINEAR_PLASTICITY. Figure 3 (a and b) shows the fracture mechanism of the cone obtained by the FEA analysis and experimental test results conducted by Kathiresan *et al.* [20]. Progressive folding fracture mechanism observed by the FEA is similar to that observed experimentally [20]. Results of model validation are presented in Table 2. Results of the FEA were found in good agreement with the results obtained experimentally by Kathiresan *et al.* [20], where the overall percentage of difference was in the range between 1.83 to 3.14%.

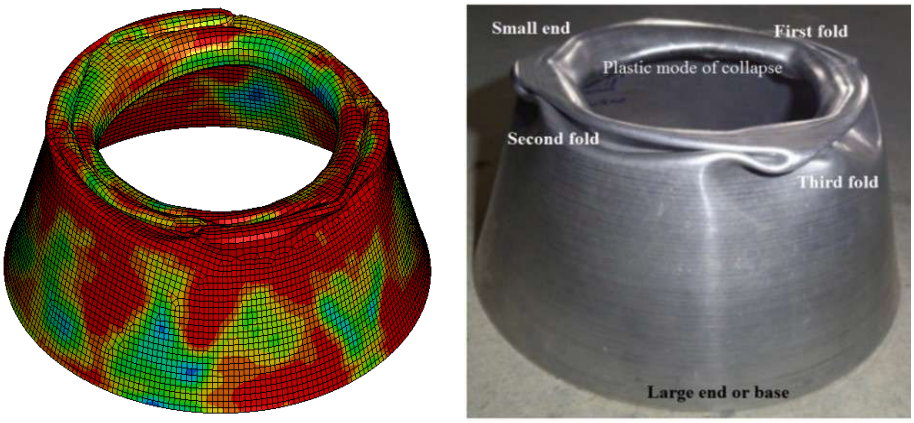

Fig. 3 *Fracture mechanism of the cone conducted by (a) FEA; (b) Experimental results*

Table 2 *Results of model validation*

Property of the material	Exp.	FEA	Percentage of difference (%)
Initial crush load (kN)	6.55	6.67	1.83
Mean Load (kN)	5.41	5.58	3.14
Maximum Load (kN)	6.75	6.89	2.07
Total absorbed Energy (J)	271.58	279.25	2.82

3.2 Crushing Characteristics

Load-displacement response of the bi-tubular components is presented in Figure 4 (a, b, c, d, and e). As shown in Figure 4, the increase in cone angle from 5° to 15° increased the initial failure load and mean crush load. The initial and mean crush load decreased with increasing cone angle to more than 15° up to 25° as shown in Figure 4(d and e). The increase in mean crushing load is attributed to the increase in the cross-sectional area of the cone with the progress in crush distance that sustains higher loads and, in turn, leads to an increase in the absorbed energy [14]. On the other hand, the increase in cone angle (α) enhances the capability of the cone to withstand higher loads and absorb higher energy on a larger cone cross-section area for the same crush distance [14]. However, there is an optimum cone angle where the crush load decreases with additional increase in the cone angle [14] [20] [21]. The decrease in crashworthiness performance of cone angles is attributed to buckling phenomena on the larger cone semi-apical angles that lower the crush load. The optimum cone angle depends on the material used and the wall thickness of the cone [14].

Int. Journal of Integrated Engineering Vol. 17 No. 8 (2025) p. 139-147

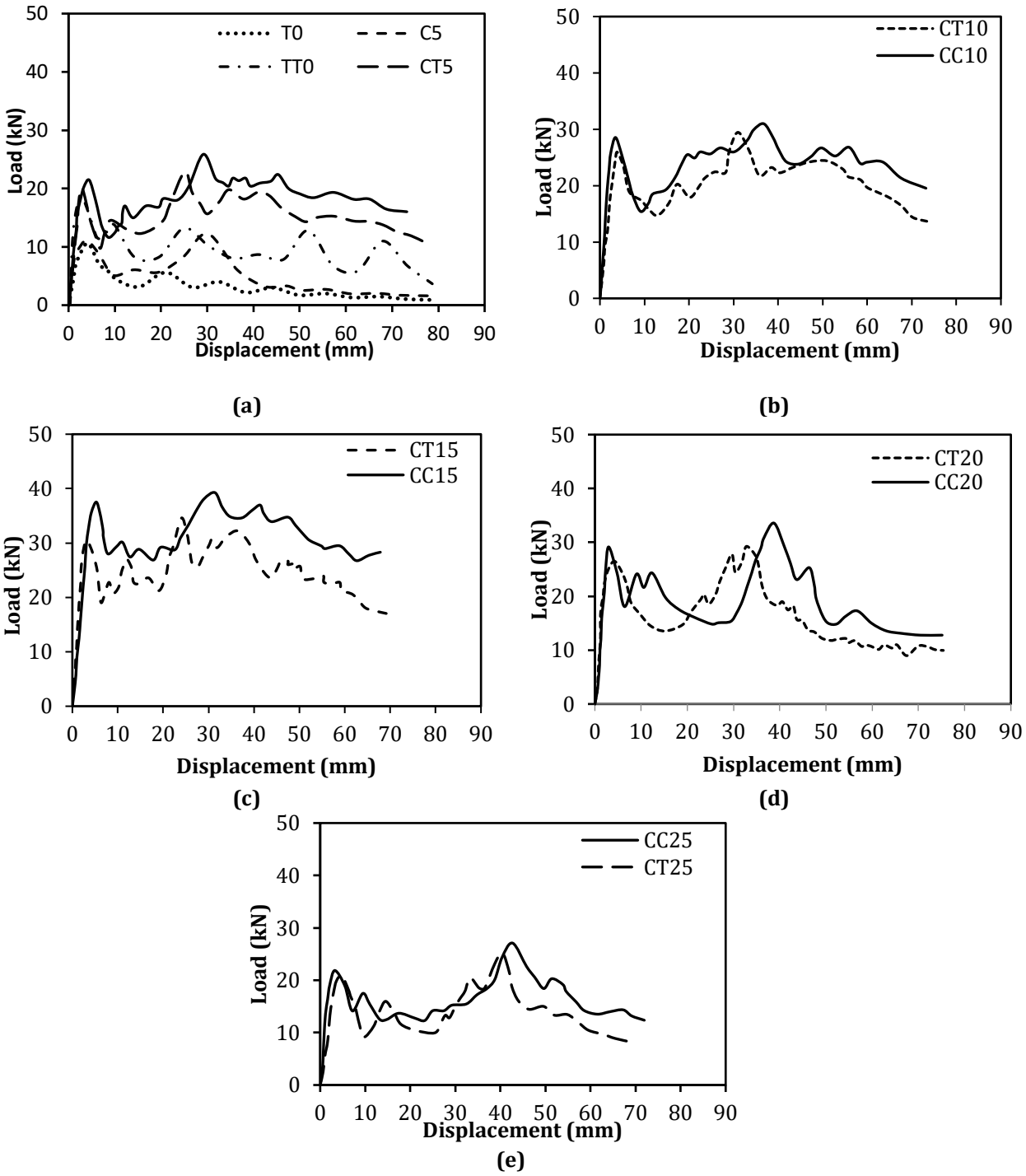

Fig. 4 *Load-displacement graphs of aluminium bi-tubular cone-cone and cone-tube for cone angles of (a) 5; (b) 10°; (c) 15°; (d) 20°; (e) 25°*

The maximum load of the tested bi-tubular components is presented in Figure 5. Increasing the cone semi-apical angle from 5° to 15° increased the load. The bi-tubular cone-cone arrangement withstands a higher load than the bi-tubular cone-tube, which is due to the increase in the cross-sectional area of the bi-tubular cones with the crush distance. Bi-tubular cones withstand lower loads using cone angles more than 15 °, which is attributed to the increase in fracture of the upper side of the cone vertically towards the inner direction of the cone with increasing the cone semi-apical angle more than 15 °. Research work conducted by Kathiresan et al. [20] found that cones of semi-apical angle 16° give higher crashworthiness performance than cones of semi-apical angles larger than 16°. The authors found that the conical specimens deform towards the inner side of the top surface of the cone where the load is applied. The authors concluded that the inside surface at the top side of the cone deforms more than the outside surface. In addition, plastic failure mode formed with crush distance progress on

the conical specimen where fixed hinges formed vertically to the applied load. The fixed hinges developed with crushing progress lead to an unsymmetric (diamond) fracture mechanism [20].

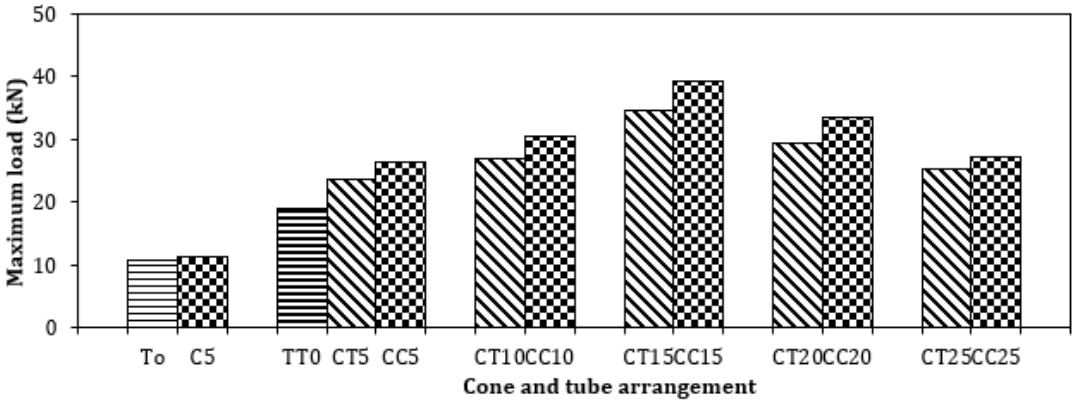

Fig. 5 *Maximum load of bi-tubular cone-cone and cone-tube*

3.3 Specific Energy Absorption

The *SEA* is a substantial factor in the crashworthiness analysis of the energy absorber system. The specific energy absorption is represented by the ratio of the total energy absorbed (*ET*) to the mass (*m*) as shown in Eq. (1) [19].

$$SEA = \frac{ET}{m} \tag{1}$$

$$\text{Where; } E_T = \int_0^{\delta_{max}} F(d\delta) \tag{2}$$

Total energy absorbed is represented by the area under the applied force-displacement relation. The crush force and displacement in the axial direction are termed by F and δ, respectively. Figure 6 shows the specific energy absorption for cone and tube arrangements.

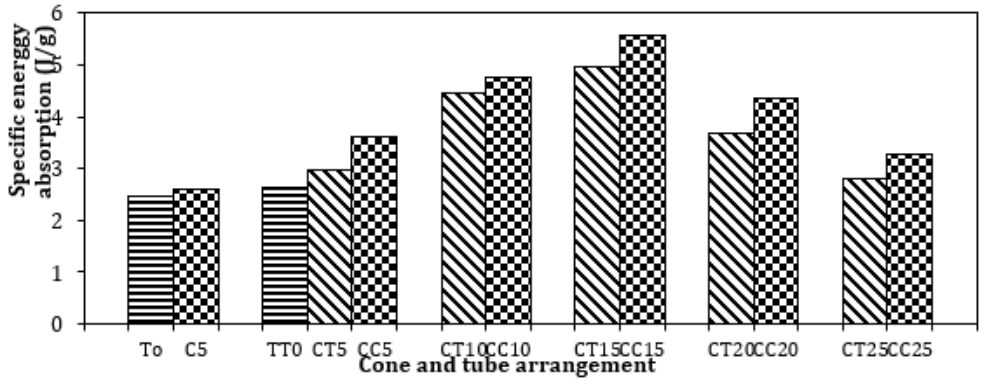

Fig. 6 *Specific energy absorption of bi-tubular cone-cone and cone-tube*

As shown in Figure 6, increasing the cone semi-apical angle up to 15 ° enhanced the absorbed energy, and it starts to decrease at a cone angle of 20°. The increase in cone angle increased the cross-sectional area of the cone, resulting in an increase in the load to be sustained by the cone, and then increased the absorbed energy. While there is an optimum cone angle that depends on material, thickness, and cross-section of the tube, where further increase in cone angle decreases the absorbed energy [14].

3.4 Mean Crush Force (*MCF*) and Crush Force Efficiency (*CFE*)

The MCF and CFE can be calculated using Eqs. (3) and (4) respectively [15].

$$MCF = \frac{\int_0^{\delta_{max}} F d\delta}{\delta_{max}} \tag{3}$$

Int. Journal of Integrated Engineering Vol. 17 No. 8 (2025) p. 139-147

$$CFE = \frac{MCF}{FM} \quad (4)$$

Results of the absorbed energy, mean, and maximum loads for bi-tubular components of different arrangements under axial loading are presented in Table 3. As shown in Table 3, combined circular tubes sustain axial load and absorb energy 43% and 6.4% higher than a single tube. Maximum load and absorbed energy of 39.26 kN and 5.58 J/g, respectively obtained on bi-tubular cones of 15° semi-apical angle (CC15). The sustained load and absorbed energy decreased to 27.08 kN and 3.27 J/g, respectively, with an additional increase in cone angle to 25°. Also, it can be noticed from Table 3 that the combined bi-tubular cone-tube (CT) withstands a lower crush load and absorbs less energy than the bi-tubular cones. As the crush distance progresses, the area of the combined cones is larger than the area of the combined cone tube.

Table 3 *Results of model validation*

Specimen	FM (kN)	MCF (kN)	ET (J)	SEA (J/g)	CFE (%)
T0	10.64	7.27	300	2.48	68.33
TT0	18.81	13.38	580	2.65	71.13
C5	12.25	8.5021	322	2.60	69.40
CT5	23.63	17.52	750	2.98	74.14
CC5	26.26	19.86	900	3.63	75.63
C10	12.66	9.13	345	2.80	72.12
CT10	27.02	20.63	1150	4.47	76.35
CC10	30.45	23.45	1260	4.77	77.01
C15	18.23	13.64	400	3.15	74.82
CT15	34.58	27.36	1300	4.96	79.12
CC15	39.26	33.27	1500	5.58	84.74
C20	16.71	11.22	423	3.23	67.15
CT20	29.24	21.02	1000	3.69	71.89
CC20	33.58	24.86	1200	4.35	74.03
C25	14.71	9.72	350	2.89	66.08
CT25	25.24	17.02	781	2.81	67.43
CC25	27.08	19.06	934	3.27	70.38

3.5 Failure Mode

The level of damage and the failure mode can be represented by the Von Mises stress contours. During the progress in the crushing process, geometrical changes lead to an increase in the stress on the bi-tubular cones and then influence the failure mode. Where the stresses at the top side of the cone are higher than the stresses at the bottom side. Table 4 shows the failure mechanism of aluminum bi-tubular cones and cone-tubes for cone semi-apical angles of 5°, 10°, 15°, 20° and 25°. Progressive folding failure mode is obtained for the fractured aluminum tubes and cones. In addition, the increase in cone semi-apical angle (α) angle more than 15 ° resulted in buckling at the bottom side of the aluminum cones that decreased the mean crushing load and absorbed energy in the region after the initial failure load. As shown in Table 4, during the compression process, the upper side of the bi-tubular cones buckled at first toward the inside and formed axi-symmetric rings or a concertina plastic failure mode. Then, fixed hinges were observed vertical to the direction of the applied load, resulting in a non-symmetric diamond failure mode.

Table 4 *Failure mode of the bi-tubular cones*

Cone semi--apical angle	5°	10°	15°	20°	25°
CC	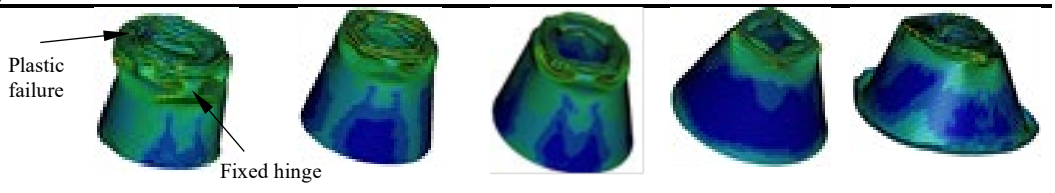				

Cone semi--apical angle	5°	10°	15°	20°	25°
CT		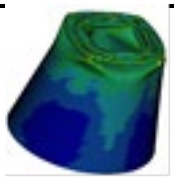		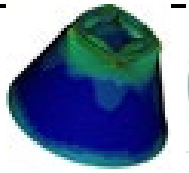	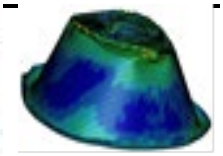

4. Conclusions

Results show that the load increased linearly for all the bi-tubular cone-tube and con-cone arrangements until their ultimate value, and then dropped and fluctuated by progressive folding mechanism till failure for the single tube and combined tubes under axial compression. Aluminum bi-tubular cones and cone-tubes withstand more force and absorb higher energy with the increase in cone angle from 5° to 15°. Increasing the cone angle to 20° and up to 25° decreased the absorbed energy, and the bi-tubes withstand lower loads.

Increasing cone angle up to 15°. Increased initial failure load from 20.04 kN to 30.50 kN and from 23.17 kN to 37.53 kN for the bi-tubular cones and cone-tube arrangements, respectively.

In general, the bi-tubular cones supported slightly higher loads than the bi-tubular cone-tube for the tested cone semi-apical angles of 5° to 25°. The summation of the loads and energies obtained from single cones and or tubes under axial crushing supported lower loads and absorbed energy than the bi-tubular cones and cone-tubes. The use of bi-tubular combinations improved the load capacity and energy absorption. Progressive folding failure mode accompanied by buckling is observed on the tested cone-cone and cone-tube arrangements. Buckling at the bottom side of the aluminum cones is observed for cone angles more than 15 °. Buckling of the upper surface of the cone towards the inside is observed, resulting in a concertina plastic fracture mechanism. With the progress in the compression process, fixed hinges were formed in a vertical direction to the applied load, leading to a non-symmetric diamond fracture mechanism.

Acknowledgement

The Authors would like to acknowledge the Faculty of Engineering at Universiti Teknologi Brunei for providing the necessary equipment and software required to conduct the current research.
(This research was not funded by any grant.)

Conflict of Interest

The authors declare that there is no conflict of interest regarding the publication of the paper.

Author Contribution

The authors confirm contribution to the paper as follows: ***study conception and design:*** *Asad A Khalid, Murhamdilah Murni;* ***data collection:*** *Asad A Khalid;* ***analysis and interpretation of results:*** *Asad A Khalid;* ***draft manuscript preparation:*** *Asad A Khalid, Murhamdillah Murni. All authors reviewed the results and approved the final version of the manuscript.*

References

[1] Gupta N. K. & Abbas H. (2000). Lateral collapse of composite cylindrical tubes between flat platens, *International Journal of Impact Engineering, 24(4)*, 329–346, https://doi.org/10.1016/S0734-743X(99)00173-6

[2] Guillow S. R., Lu G. & Grzebieta R. H (2001). Quasi-static axial compression of thin-walled circular aluminium tubes, *Intërnational Journal of Mechanical Sciences, 43(9)*, 2103–2123, https://doi.org/10.1016/S0020-7403(01)00031-5

[3] Al Galib D., & Limam A. (2004). Experimental and numerical investigation of static and dynamic axial crushing of circular aluminum tubes, *Thin-Walled Structures, 42(8)*, 1103–1137, https://doi.org/10.1016/j.tws.2004.03.001

[4] Langseth M., & Hopperstad O. S. (1996). Static and dynamic axial crushing of square thin-walled aluminium extrusions," *International Journal of Impact Engineering, 18(7-8)*, 949–968, https://doi.org/10.1016/S0734-743X(96)00025-5

[5] El-Hage H., Mallick P. K., & Zamani N. (2004). Numerical modelling of quasi-static axial crush of square aluminium-composite hybrid tubes, *International Journal of Crashworthiness, 9(6)*, 653–664, https://doi.org/10.1533/ijcr.2004.0320

[6] El-Hage H., Mallick P. K., & Zamani N.(2006). A numerical study on the quasi-static axial crush characteristics of square aluminum - Composite hybrid tubes, *Composite Structures, 73(4)*, 505–514, https://doi.org/10.1016/j.compstruct.2005.03.004

[7] Haghi Kashani M., Shahsavari Alavijeh H. Akbarshahi H., & Shakeri M. (2013). Bitubular square tubes with different arrangements under quasi-static axial compression loading, *Materials and Design, 51*, 1095–1103, https://doi.org/10.1016/j.matdes.2013.04.084

[8] Praveen Kumar A., Pradeep C., Sai Rahul Gupta S., Vamshi Krishna G., & Harshavardhan G. (2021). Impact loading behavior of woven glass fabric polymer composite bi-tubular square sections, *Materials Today Proceedings, 47(17)*, 6291–6295, https://doi.org/10.1016/j.matpr.2021.05.529

[9] Praveen Kumar A. and Nageswara Rao D. (2021). Crushing characteristics of double circular composite tube structures subjected to axial impact loading, *Materials Today Proceedings, 47(17)*, 5923–5927, https://doi.org/10.1016/j.matpr.2021.04.465

[10] Praveen Kumar A., Yadi Reddy M. & Shunmugasundaram M., (2021). Energy absorption analysis of novel double section triangular tubes subjected to axial impact loading, *Materials Today Proceedings, 47(17)*, 5942–5945, https://doi.org/10.1016/j.matpr.2021.04.485

[11] Praveen Kumar A. & Sravani D.(2021). Experimental assessment of axial deformation behaviour of aluminium-kevlar composite hybrid bitubular structures, *Materials Today Proceedings, 47(17)*, 5955–5958, https://doi.org/10.1016/j.matpr.2021.04.492

[12] Nagel G. M., & Thambiratnam D. P. (2004). A numerical study on the impact response and energy absorption of tapered thin-walled tubes, *International Journal of Mechanical Sciences, 46(2),* 201–216, https://doi.org/10.1016/j.ijmecsci.2004.03.006

[13] Nagel G. M., & Thambiratnam D. P. (2005). Computer simulation and energy absorption of tapered thin-walled rectangular tubes, *Thin-Walled Structures, 43(8)*, 1225–1242, https://doi.org/10.1016/j.tws.2005.03.008

[14] Asad A Khalid, Barkawi Sahari, & Khalid Y. A. (2002). Performance of composite cones under axial compression loading, *Composits Science and Technology,* 62(1), 17–27, https://doi.org/10.1016/S0266-3538(01)00092-6

[15] Livermore software technology corporation (LSTC), (2009). *LS-DYNA Keyword User ' S Manual,* Version 971 / Release 4, Beta, I.

[16] Klaus-JuÈrgen Bathe, Jan Walczakb, Olivier Guillermin, Pavel A. Bouzinov, & Heng-Yee Chen. (1999). Advances in crush analysis, *Computers and Structures, 72(1)*, 31–47, https://doi.org/10.1016/S0045-7949(99)00041-3

[17] El-Hage H., Mallick P. K., & Zamani N. (2010). A numerical study on the quasi-static axial crush characteristics of square aluminum tubes with chamfering and other triggering mechanisms, *International Journal of Crashworthiness 10(2)*, 183-196, https://doi.org/10.1533/ijcr.2005.0337

[18] Haipeng Han, Farid Taheri, Neil Pegg, & You Lu. (2007). A numerical study on the axial crushing response of hybrid pultruded and ±45° braided tubes, *Compos. Struct.*, *80(2)*, 253–264, https://doi.org/10.1016/j.compstruct.2006.05.012

[19] Mehmet A. Guler, Muhammed E. Cerit, Bertan Bayram,Bora Gerçeker, & Emrah Karakaya. (2010). The effect of geometrical parameters on the energy absorption characteristics of thin-walled structures under axial impact loading, *Int. J. Crashworthiness*, *15(4)*, 377–390, https://doi.org/10.1080/13588260903488750

[20] Kathiresan M., Manisekar K., & Manikandan V. (2012). Performance analysis of fibre metal laminated thin conical frusta under axial compression, *Composite Structures, 94(12)*, 3510–3519, https://doi.org/10.1016/j.compstruct.2012.05.026

[21] Price JN., & Hull D. (1987). Axial crushing of glass fiber polyester composite cones, *Composite Science and Technology, 28*, 211–330, https://doi.org/10.1016/0266-3538(87)90003-0